Original Research

In vitro and *in vivo* clearance of Rose Bengal Acetate-PhotoDynamic Therapy-induced autophagic and apoptotic cells

Elisa Panzarini, Valentina Inguscio, Bernardetta Anna Tenuzzo and Luciana Dini

Department of Biological and Environmental Science and Technology (Di.S.Te.B.A.), University of Salento, 73100 Lecce, Italy
Corresponding author: Luciana Dini. Email: luciana.dini@unisalento.it

Abstract

This study focuses on the clearance of Rose Bengal Acetate (RBAc)-PhotoDynamic Therapy (PDT)-generated apoptotic and autophagic HeLa cells by murine and human macrophages. Indeed, phagocytosis of dead cells drives the therapeutic efficacy of PDT through both efficient removal of dead/dying cells and macrophages response evoked during engulfment and, up to now, clearance of dying photosensitized cells has been less investigated than PDT mechanisms of cell death induction. RBAc-PDT ensures a long onset of cytotoxicity and a time-related cell death of HeLa cells by signals originating from or converging on almost all intracellular organelles. On this basis, to clarify whether the efficacious cell death commitment is followed by an efficient clearance mechanism, we primarily focused on the analysis of 'eat me' signals exposure and 'find me' signals release, and then investigated the migration, recognition, engulfment and response of murine Raw 264.7 and human blood isolated macrophages.

Dead cells secreted 'find me' signals, i.e. fractalkine and Heat Shock Protein 70 (HSP 70), to recruit macrophages and promote their fast phagocytosis. Macrophages phagocytosed apoptotic and autophagic PDT-treated cells more efficiently than the respective positive controls, i.e. puromycin-induced apoptotic and Earle's balanced salt solution-starved autophagic cells. Phagocytosis depends on the glycans exposed on dead cells. The macrophages internalization of photokilled cells elicits the production of Interleukin-10, Transforming Growth Factor-β and Tumour Necrosis Factor-α by macrophages. TNFα production, along with HSP70 release and plasma membrane translocation on dead cells, suggest an immunogenic impact of RBAc-PDT. In fact, macrophages, activated fibroblasts and endothelial cells colonized the inoculum site of photosensitized cells in rat calf muscles, endorsing the hypothesis of immunogenic elicitation of RBAc-PDT.

Keywords: phagocytosis, rose bengal acetate, photodynamic therapy, cytokines, fractalkine, HSP70

***Experimental Biology and Medicine* 2013; 238: 765–778. DOI: 10.1177/1535370213494552**

Introduction

PhotoDynamic Therapy (PDT), Food and Drug Administration-approved treatment for malignant and non-diseases, is an emerging cancer protocol used to eradicate premalignant and early-stage cancer and to reduce the tumour size in end-stage cancers. PDT kills neoplastic cells via cytotoxicity elicited by particular drugs, called Photo-Sensitizers (PSs), able to preferentially accumulate in the cancerous tissue.[1] Upon irradiation with visible light of a wavelength matching its absorption spectrum (therapeutic window: 600–800 nm), the PS induces direct Reactive Oxygen Species (ROS)-mediated photodamage of tumour cells,[2] resulting in a cascade of oxidative events that induce extensive cell death through several mechanisms, i.e. apoptosis, necrosis and autophagy, as suggested by different *in vitro* and *in vivo* studies.[3,4] In addition, PDT can indirectly lead to tumour eradication by blocking blood supply in tumour area or by eliciting tumouricidal activity of immune effectors recruited in the tumour area by dead/dying cells.[5] Indeed, in this context, the fate of the massive presence of dead/dying cells may have a critical impact on cancer therapy. In fact, dead/dying cells play a controversial role also in normal tissue, where by perpetuating active inflammation they may provide an immunogenic impetus for the onset of disorders, such as lupus systemic erythematosus, cystic fibrosis, chronic obstructive pulmonary disease,[6–9] or they can impair tissue integrity. The role of removal of dead/dying cells in cancer is becoming clear, since both innate and adaptive immune system cell types can influence cancer onset, development and resolution.[10]

In vivo, apoptotic cells are quickly removed by phagocytes in a complex and dynamic process divided in distinct steps: attraction and accumulation of phagocytes to the site

of apoptotic cells ('find me' signals-mediated), recognition and tethering ('eat me' signals-mediated) and internalization and processing of dead cells within the phagocytes, that in turn produce and release soluble molecules, e.g. immunomodulatory cytokines, that elicit tolerogenic or immunogenic response. The balance between immunogenic and tolerogenic cell death/clearance depends on the phagocytic cell type, i.e. dendritic cells or macrophages, and the factors released.[11,12] The hallmark feature of apoptotic cell clearance is the non-inflammatory nature of this process. However, there are exceptions in which apoptotic cells can elicit an immune response. For examples, engulfment of oncogenic cells can play a role in the presentation of altered self-peptides, that may be presented to the immune system.[13] In addition, recently several papers report the ability of apoptotic tumour cells to ignite a robust immune response[14] by exposure or release of molecule, called Damage-Associated Molecular Patterns (DAMPs), e.g. calreticulin, involved also in phagocytosis by dendritic cells.[15]

Several molecular elements, such as phagocytosis receptors, cell surface molecules, bridging molecules, signal transducers, engulfment proteins, effector molecules, transcription factors and inflammatory regulators and cytokines, orchestrate the dynamic interrelationship between dying and engulfing cells.[16] The rapid and efficient phagocytosis of apoptotic cells is based on efficacious sensing mechanisms elicited by dead/dying cells and active engulfment driven by specific molecules present on plasma membrane of both phagocyting and dead/dying cells.

PDT has largely been investigated with regards to the mechanisms of the induction of cell death, but the final fate and the clearance mechanism of dying photosensitized cells have not yet been fully elucidated. Therefore, the aim of this work is to study the phagocytosis of apoptotic and autophagic HeLa cells generated by photodynamic treatment with Rose Bengal Acetate (RBAc), a powerful PS efficiently inducing apoptosis and autophagy in HeLa cells through ROS and endoplasmic reticulum stress. RBAc-PDT ensures a long onset of cytotoxicity and time-related cell death by signals originating from or converging on almost all intracellular organelles.[17–21] On this basis, to clarify whether the efficacious cell death commitment is followed by an efficient clearance mechanism, we primarily focused on the analysis of 'eat me' signals exposure and 'find me' signals release, successively investigating the migration, recognition, engulfment and response of murine Raw 264.7 and human blood-isolated macrophages.

Materials and methods

Cell cultures and animals

HeLa cells. Human cervical carcinoma HeLa cells were cultured in Eagle's minimum essential medium (EMEM; Cambrex, Verviers, Belgium) supplemented with 10% foetal bovine serum (FBS; Cambrex), 2 mmol/L L-glutamine (Cambrex), 100 IU/mL penicillin and streptomycin solution (Sigma, St. Louis, MO, USA) and 10,000 U/mL amphotericin B (antimicotic solution; Cambrex), in a 5% CO_2 humidified atmosphere at 37°C. The cells were maintained in 75 cm^2 flasks (between 2×10^5 and 1×10^6 cells/mL) by passage every 3–4 days.

Raw 264.7. The murine Raw 264.7 macrophages were cultured in Dulbecco's modified eagle medium (DMEM; Cambrex) supplemented with 10% FBS, 2 mmol/L L-glutamine, 100 IU/mL penicillin and streptomycin solution and 10,000 U/mL amphotericin B, in a 5% CO_2 humidified atmosphere at 37°C. The cells were maintained in 75 cm^2 flasks at a concentration of 5×10^5 cells/mL by passage every 3–4 days.

Cells were seeded 24 h before the experiments.

Human macrophages. Human monocytes were isolated from the 'buffy coats' of healthy blood donors on Ficoll–Paque Plus (Amersham Biosciences, Glattbrugg, Switzerland) gradients and magnetic separation using CD14 human microbeads (Miltenyi Biotec, Auburn, CA, USA). Human macrophages were obtained through five-day differentiation using 5 ng/mL macrophage colony-stimulating factor.

Rats. Male Wistar rats (150–200 g) were housed in a temperature-controlled (22 ± 1°C) animal holding room with free access to commercial rat diet and tap water. Experiments were carried out in accordance with local and national guidelines for animal experimentation.

PDT treatment

Photodynamic treatment was performed as already reported in order to induce autophagy and apoptosis at 8 (25%) and 12 h (40%) of recovery after irradiation.[19] On the basis of cell death evaluation reported by Panzarini *et al.*,[19] we chose 8 and 12 h after irradiation recovery times and the treatment was performed in the presence of apoptosis (pan-caspase inhibitor, Z-VAD-FMK, 20 μmol/L; R&D Systems, Minneapolis, MN, USA), autophagy (3-methyladenine [3-MA] 10 mmol/L; Sigma-Aldrich Chem. Co, St Louis, MO, USA) and necroptosis (necrostatin 1 [Nec-1], 300 μmol/L; Santa Cruz Biotechnology Inc., Santa Cruz, CA, USA) specific inhibitors in order to obtain autophagic and apoptotic cells fractions at 90% purity. The autophagic HeLa cells fraction was obtained by using Z-VAD-FMK and Nec-1 simultaneously; apoptotic HeLa cells fraction was obtained by using 3-MA and Nec-1. The cell death inhibitors were added 30 min before photodynamic treatment, during RBAc treatment (1 h incubation) and after irradiation during the recovery time periods (8 and 12 h), in a 5% CO_2 humidified atmosphere at 37°C.

HeLa cells treated with puromycin (PMC; 20 μmol/L, 4 h), Earle's balanced salt solution (EBSS; starvation 6 h) and heat shock (HS; 48–50°C 1 h) were used as positive control for apoptotic, autophagic and necrotic cells, respectively.

Cells were seeded 24 h before the experiments.

In vitro phagocytosis assay

Phagocytosis of autophagic and apoptotic HeLa cells was performed using Raw 264.7 cells and human macrophages as phagocytes. Twenty-four hours before the phagocytosis assay, 2×10^5 Raw 264.7 cells and human macrophages were seeded on coverslips, in a six-well plate. Both Raw 264.7 cells and human macrophages were incubated with autophagic and apoptotic HeLa cells in a ratio of 10:1 (10 dead cells per phagocyte) for 4 h at 37°C. Dead cells were stained with 1 μg/mL Hoechst 33342 for 5 min at 37°C before being added to the macrophage cultures. In inhibition experiments, a mixture of galactose/*N*-acetylglucosamine/mannose/*N*-acetylgalactosamine/fucose (80 mmol/L final concentration) was used.

The phagocytosis rate (number of macrophages engulfing at least one autophagic or apoptotic cell) and phagocytosis index (number of autophagic or apoptotic cells internalized per macrophage) were reported by scoring at least 500 cells for each experiment, under a fluorescence microscope NIKON Eclipse 80i (Nikon, Tokyo, Japan), with Plan Fluor objectives (Nikon). The percentage of cells binding but not ingesting autophagic or apoptotic cells was calculated and expressed as percentage of binding.

In situ adhesion experiments

Eight male Wistar rats (150–200 g) were anaesthetized by an intraperitoneal injection of sodium thiopental (10 mg/100 mg body weight; Farmotal, PHARMACIA & UPJOHN S.p.A., Milano, Italy).

The livers were perfused in a non-recirculating system at a flow rate of 1 mL/min. A concentration containing 1×10^6 dead HeLa cells were injected into the liver circulation (total volume 1 mL) following the protocol described by Dini *et al*.[22] The HeLa cells used in the different experiments were either viable, apoptotic and autophagic PDT-induced or apoptotic PMC-induced. The livers were extensively washed with culture medium to remove unbound cells; then, they were fixed in 4% paraformaldehyde in phosphate buffer and finally processed for routine light microscopy. In control experiments, the livers were perfused with a mixture of galactose/*N*-acetylglucosamine/mannose/*N*-acetylgalactosamine/fucose (80 mmol/L final concentration) before administration of the dead HeLa cells.

The adhesion and internalization of HeLa cells by the sinusoidal cells were evaluated by using an Eclipse 80i light microscope after haematoxylin–eosin staining, by counting the number of hepatic sinusoidal endothelial (HSE) and Kupffer cells (KCs) of the periportal (pp) and perivenous (pv) region binding and internalizing apoptotic and autophagic HeLa cells per mm^2. All reagents used in these experiments were refrigerated at 4°C, in order to mainly evaluate the adhesion and limit the internalization both by HSE and KCs.

Lectin binding to the plasma membrane

Cell surface glycans exposure was analysed at fixed times post PDT on both the attached and suspension dead cells by using fluorescein isothiocyanate (FITC)-conjugated lectins (Sigma-Aldrich, St. Louis, MO, USA) with different specificities: 40 μg/mL concanavalin A (ConA; α-D-mannose [α-man]), 2 μg/mL *Ricinus communis* (RCA; β-D-galactose), 60 μg/mL *Helix pomatia* (HPA; *N*-acetyl-D-galactosamine [galNAc]), 50 μg/mL *Lycopersicon esculentum* (*N*-acetyl-D-glucosamine [glcNAc] and *N*-acetyl-lactosamine [lacNAc]) and 60 μg/mL *Phytolacca americana* (glcNAc), 40 μg/mL *Ulex europaeus* (α-L-fucose) and 120 μg/mL *Triticum vulgaris* (*N*-acetyl-β-D-glucosaminyl residues and glcNAc oligomers/sialic acid). Cells were incubated with lectins for 30 min in the dark. Labelling was observed with a fluorescence microscope Eclipse 80i.

ELISA assay for fractalkine

The soluble form of fractalkine (FKN) was detected in the cell supernatants of HeLa cells induced to death with the different treatments, using the DuoSet enzyme-linked immunosorbent assay (ELISA) following manufacturer instructions (R&D Systems). The optical density of each well was immediately determined at 450 nm by using the microplate reader Thermo electron corporation MULTISKAN EX ORIGINAL (Thermo Fisher Scientific Inc., Waltham, MA, USA).

Chemotaxis assay

The human and Raw 264.7 macrophages chemotaxis assay was performed using polyester (PET) transwells (8-μm pore size; BD Falcon, BD Biosciences, Erembodegem, Belgium). After RBAc-PDT, PMC, HS and EBSS treatments, HeLa cells were seeded on the lower well of chamber and were co-cultured for 3 h with macrophages seeded on the upper well of the chamber. The percentage of macrophage migration was calculated on haematoxylin–eosin stained macrophages seeded on the upper chamber of transwells. We separately counted the number of cells localized on the upper surface, in the pores and on the lower surface of a 8 μm pore-size transwells. In the control experiment, recombinant human and murine FKN (60 pg/mL; R&D Systems) was added to the culture medium of the low chamber of the transwells instead of dead HeLa cells. Anti-FKN monoclonal antibody (50 μg/mL; R&D Systems) was added to the cultures of living or dead HeLa cells 30 min before the transfer of the inserts and throughout the entire assay in other experiments.

Immunoblot analysis of HSP70 protein

At fixed times post PDT, purified plasma membrane proteins of HeLa cells were obtained according to the Plasma Membrane Protein Extraction Kit instructions (BioVision, Mountain View, CA, USA), while the culture medium in which the experiments were performed was collected and proteins were precipitated in acetone.

Immunoblotting analysis. The proteins (30 μg) were resolved in 13% sodium dodecyl sulphate polyacrylamide gel electrophoresis (SDS-PAGE; Bio-Rad Laboratories, Hercules, CA, USA). For immunoblotting analysis, the proteins were transferred to a nitrocellulose membrane. The membranes were blocked for 1 h in Tris-buffered saline

(TBS) 25 mmol/L pH 8.3/3% bovine serum albumin (BSA). The monoclonal heat shock protein 70 (HSP70) primary antibody (Sigma-Aldrich), diluted 1:2000, was incubated with the membrane. Appropriate IgG biotin-conjugated secondary antibody (Sigma-Aldrich), diluted 1:2000, was incubated with the membranes for 2 h. Membranes were then incubated with ExtrAvidin peroxidase (Sigma-Aldrich) diluted 1:1500 at 4°C for 1 h. After each incubation with antibody and prior to the addition of diaminobenzidine solution for 20 min at dark, membranes were washed three times in TBS 25 mmol/L pH 8.3. The densitometer analysis was performed using GS-700 Imaging Densitometer (Bio-Rad).

The monoclonal e-cadherin primary antibody (Sigma-Aldrich) and actin primary antibody (Sigma-Aldrich), diluted 1:2000, were used as control.

Cytokines release

To detect Interleukin-10 (IL10), Transforming Growth Factor-β (TGFβ) and Tumour Necrosis Factor-α (TNFα) production by human and Raw 264.7 macrophages, the supernatants of the phagocytosis and chemotaxis assays were collected and subjected to ELISA analysis, using the DuoSet ELISA Development System manufactured by R&D Systems according to the manufacturer protocol. Raw 264.7 macrophages stimulated by lipopolysaccharide (LPS, 1 mg/mL; Sigma-Aldrich) and interferon-γ (IFNγ, 100 UI/mL; Sigma-Aldrich) for 24 h were used as positive controls.

In vivo experiments

A total of 36 male Wistar rats were sedated with ether anaesthesia and divided in 12 groups according to the inoculation types, reported below performed in bilateral anterior and posterior calf muscles of each rat. Inoculation volume was 500 μL and cell number 5×10^5. Rats were sacrificed at 3, 7 and 15 post-inoculation (PI) days.

Inoculation types: sterile pyrogen free water; viable HeLa cells; EMEM (10% FCS); 5×10^5 latex beads; necrotic HS (48–50°C 1 h)-induced HeLa cells; autophagic starvation (EBSS 6 h)-induced HeLa cells; autophagic starvation (EBSS 6 h)-induced HeLa cells conditioned medium; apoptotic PMC (20 μmol/L 4 h)-induced HeLa cells; 6 pg of FKN; autophagic and apoptotic RBAc-PDT-induced HeLa cells; autophagic and apoptotic RBAc-PDT-induced HeLa cells conditioned medium.

Immunohistochemistry of muscle tissue sections. The muscles were explanted and fixed by immersion in 4% paraformaldehyde for 2 h, and were then dehydrated and embedded in 54°C paraffin. Three micrometre-thick sections were cut by using a microtome Reichert-Jung 2050 Supercut (Leica Microsystems GmbH, Wetzlar, Germany). Immunohistochemistry of CD68 and type II TGFβ receptor was performed on muscle sections placed onto gelatine-coated slides. Anti-CD68 antibody recognizes tissue macrophages, fibroblasts and activated endothelial cells, while the anti-type II TGFβ receptor antibody recognizes fibroblasts and activated endothelial cells, thus suggesting a recruitment of macrophages and an inflammatory reaction, respectively. Endogenous peroxidase activity was quenched by treating the sections with 3% H_2O_2 in methanol for 20 min at room temperature. The slides were incubated with 0.5% trypsin in TBS for 5 min at 37°C for antigen retrieval and then with blocking solution (1% BSA in TBS) for 20 min in a humidified chamber to block excess proteins and prevent non-specific antibody binding. Sections were incubated with the primary antibodies (Santa Cruz Biotechnology), anti-type II TGFβ diluted 1:100, final concentration of 2 μg/mL and anti-CD68 diluted 1:10, final concentration of 90 μg/mL in the blocking solution for 60 min at room temperature in a humidified chamber. Slides were washed two times with TBS and incubated with a biotinylated secondary antibody (diluted 1:50 in blocking solution, final concentration of 5 μg/mL) for 60 min at room temperature in a humidified chamber. The slides were then washed two more times with TBS before incubation with an avidin–biotin complex (ABC; Vector Laboratories Inc., Burlingame, CA, USA) for 15 min at room temperature in a humidified chamber. Immunoreactivity, indicated by the appearance of brown colour, was developed with 0.05% of 3,3′-diaminobenzidine tetrahydrochloride (Sigma-Aldrich) in 0.1% H_2O_2 in TBS for 3 min. Sections were rinsed in distilled water and counterstained with haematoxylin and processed for light microscope observation using an Eclipse 80i light microscope. The number of cells positive to immunostaining was calculated and reported per mm^2.

The specificity of immunostaining was controlled by omitting incubation with the primary or secondary antibodies or both of them.

Statistical analysis

The two-tailed Student's *t*-test was used to analyse the differences between the controls and treated samples. Data are presented as a mean value ± SD and all tests were performed at the 0.05 significance level.

Results

Cell surface modifications

RBAc-PDT causes a rearrangement of sugar residues on the plasma membrane of apoptotic and autophagic HeLa cells compared to apoptotic PMC-induced and autophagic EBSS-induced HeLa cells, suggesting cell death inducer and type-dependent differences in amount, distribution and type of glycan residues. galNAc, glcNAc, lacNAc and β-D-gal residues are highly exposed on the surface of photosensitized apoptotic HeLa cells while α-man residues are highly exposed on photosensitized autophagic ones. A handful of glycans residues characterized the surface of EBSS-starved HeLa cells. Sialic acid is remarkably exposed on apoptotic PMC-induced HeLa cells (Figure 1a,b).

Binding and internalization of dead HeLa cells

In vitro. In reporting all the data, we will refer to 'macrophages' for both human and murine cells, since, although human macrophages are most efficient at phagocytosing dead cells, the trend of results is similar (see Table 1 for the respective absolute values). Macrophages bind and

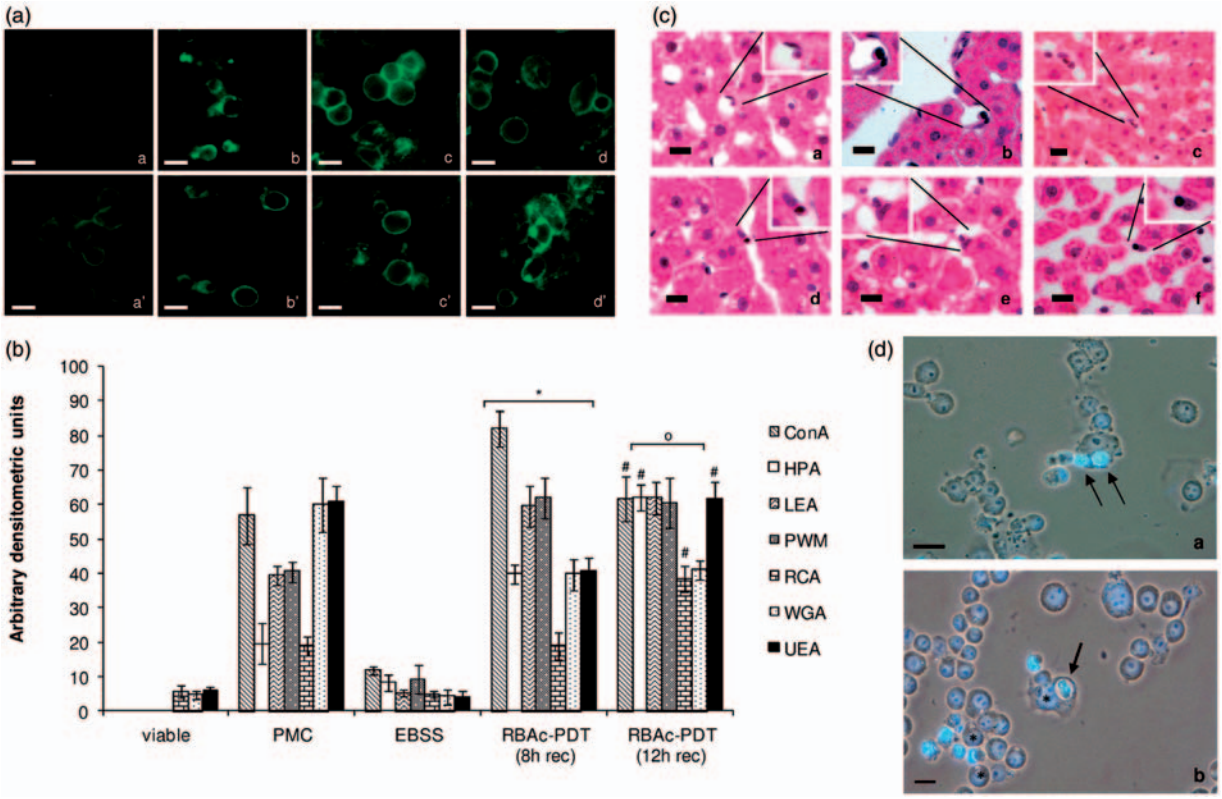

Figure 1 Cell surface glycans modification of apoptotic and autophagic RBAc-PDT induced HeLa cells and phagocytosis by human and murine macrophages
a: Fluorescence micrographs of viable (a–a'), puromycin (PMC) 20 μmol/L 4 h (b–b'), RBAc-PDT 8 (c–c') and 12 h (d–d') of recovery post PDT HeLa cells labelled with FITC conjugated lectins (a-d: *Concanavalin A*; a'–d': *Triticum vulgaris*). HeLa cells were incubated 60 min with rose bengal acetate 10^{-5} mol/L followed by 90 s irradiation with green light (1.6 J/cm^2) and by 8 and 12 h of recovery in fresh medium. Bars = 10 μm
b: Quantitative fluorescence cell image analysis (fluorescence expressed as arbitrary absorbance units) of glycans residues exposed on HeLa cells plasma membrane. The data are the mean ± SD of three independent experiments
Viable: untreated HeLa cells; PMC: apoptotic PMC (20 μmol/L 4 h)-induced HeLa cells; EBSS: autophagic starvation (EBSS 6 h)-induced HeLa cells; RBAc-PDT (8 h rec): autophagic PDT-induced HeLa cells; 8 h of recovery post PDT; RBAc-PDT (12 h rec): apoptotic PDT-induced HeLa cells, 12 h of recovery post PDT; RBAc-PDT: HeLa cells incubated with rose bengal acetate for 60 min followed by 90 s irradiation with green light (1.6 J/cm^2) and then by recovery in fresh medium (8 and 12 h); ConA: concanavalin A (α-D-mannose); HPA: *Helix pomatia* (*N*-acetyl-D-galactosamine); LEA: *Lycopersicon esculentum* (*N*-acetyl-D-glucosamine, *N*-acetyl-lactosamine); PWM: *Phytolacca americana* (*N*-acetyl-D-glucosamine); RCA: *Ricinus communis* (β-D-galactose); WGA: *Triticum vulgaris* (*N*-acetyl-β-D-glucosaminyl residues and *N*-acetyl-β-D-glucosamine oligomers/sialic acid); UEA: *Ulex europaeus* (α-D-fucose). *Values significantly different ($P < 0.05$) with respect to EBSS values; °values significantly different ($P < 0.05$) with respect to PMC values; #values significantly different ($P < 0.05$) between autophagic and apoptotic photosensitized values
c: Light microscope micrographs of haematoxylin–eosin stained paraffin sections of rat livers injected with RBAc-PDT-treated cells at 12 h of recovery (a, d), RBAc-PDT-treated cells at 8 h of recovery (b, e) and PMC 20 μmol/L 4 h (c, f) HeLa cells. In (a–c) dead HeLa cells bound to hepatic sinusoidal cells; in (d–e) dead HeLa cells internalized by hepatic sinusoidal cells. Bars = 10 μm
d: Phase contrast micrographs of Hoechst 33342 (1 μg/mL) labelled dead HeLa cells co-incubated with Raw 264.7 macrophages. HeLa cells were induced to death by RBAc-PDT 8 (a) and 12 h (b) of recovery post PDT. Internalizations (arrows) or binding (asterisks) to Raw 264.7 macrophages are shown. Bars = 10 μm.
(A color version of this figure is available in the online journal)

ingest photokilled cells more efficiently than PMC-treated ones and preferentially tether and tickle apoptotic PDT-treated HeLa cells better than autophagic PDT-treated HeLa cells (Figure 1d). Indeed, a hierarchy of binding to macrophages was observed: autophagic and apoptotic PDT-induced more than PMC-induced and EBSS-starved HeLa cells.

The engulfment of dead cells bound to the surface of macrophages was quick and efficient and starts as soon as after 30 min/1 h of co-incubation with a peak at 3 h (data not shown), a time chosen for all of the phagocytosis experiments. However, the rate but not the index of phagocytosis relies on the type of death, i.e. autophagic or apoptotic, and on the cell death inducer, i.e. PDT, PMC and EBSS starvation (Table 1). Macrophages engulf more apoptotic PDT-generated cells than autophagic ones, and more apoptotic PDT-induced cells than PMC-induced ones. Autophagic EBSS-starved cells are engulfed at the lowest rate. Binding and internalization of PDT-generated HeLa cells are significantly affected by competing sugars (>80% of reduction; data not shown).

In situ. Once injected into the hepatic circulation of male Wistar rats, photokilled apoptotic and autophagic HeLa cells are very efficiently removed by the HSEs and KCs of the pp region (80% of the dead cells) and to a lesser extent by the pv region cells (20% of the dead cells; Table 2). Differences of binding and engulfment are found between

Table 1 Phagocytosis index and rate, percentage of binding and number of apoptotic and autophagic HeLa cells bound per isolated human (H) and murine Raw 264.7 (M) macrophages

HeLa cells co-cultured with macrophages	Phagocytosis Index		Phagocytosis Rate (%)		Number of dead cells bound/macrophage		Binding (%)	
	H	M	H	M	H	M	H	M
Viable	N.D.	N.D.	N.D.	N.D.	N.D.	N.D.	N.D.	N.D.
PMC 4h	1,65 ± 0,15	1,1 ± 0,1	11,25 ± 2,7	7,5 ± 1,3	2,72 ± 0,16	1,7 ± 0,1	37,6 ± 2,7	23,5 ± 1,7
RBAc-PDT (12h rec)	1,95 ± 0,45	1,3 ± 0,3	22,05 ± 3,1*	14,7 ± 2,5*	3,68 ± 0,32*	2,3 ± 0,2*	46,24 ± 2,4*	28,9 ± 1,5*
EBSS 6h	1,8 ± 0,75	1,2 ± 0,5	7,65 ± 1,3	5,1 ± 1,1	1,92 ± 0,96	1,2 ± 0,6	12,48 ± 4,1	7,8 ± 2,5
RBAc-PDT (8h rec)	1,65 ± 0,3	1,1 ± 0,2	14,55 ± 2,9*°	9,7 ± 2,1*°	3,36 ± 0,48*°	2,1 ± 0,3*°	40,48 ± 2,08°	25,3 ± 1,3°

Phagocytosis index: number of dead cells internalized per macrophage.
Phagocytosis rate: number of macrophages internalizing at least one dead cell.
Percentage of binding: number of macrophages binding at least one dead cell.
Viable: untreated HeLa cells; PMC 4h: apoptotic puromycin (20 μM 4h)-induced HeLa cells; RBAc-PDT (12h rec): apoptotic PDT-induced HeLa cells, 12 h of recovery post PDT; EBSS 6h: autophagic starvation (EBSS 6h)-induced HeLa cells; RBAc-PDT (8h rec): autophagic PDT-induced HeLa cells, 8 h of recovery post PDT.
N.D. Not Detected value, corresponding to 0 cells counted
RBAc-PDT: HeLa cells incubated with Rose Bengal Acetate for 60 min followed by 90 seconds irradiation with green light (1.6 J/cm^2) and then by recovery in fresh medium (8 and 12 h).
Each value is the average +SD of 500 cells scored out of three independent experiments.
*Values significantly different ($p < 0.05$) with respect to the PMC 20 μM 4h.
°Values significantly different ($p < 0.05$) with respect to the EBSS 6h.

KCs and HSEs of the same hepatic region (KCs internalize dead cells 1.5-fold more than HSEs) and are related to the dead cell type. In fact, apoptotic and autophagic PDT-induced HeLa cells are, respectively, internalized 2.4- and 2.3-fold more than apoptotic PMC-induced cells. KCs preferentially bind photokilled HeLa cells while HSEs 'prefer' apoptotic PMC- or PDT-induced HeLa cells more than autophagic cells (Table 2; Figure 1c). Table 2 reports the number of HSEs and KCs of pp and pv region binding and internalizing apoptotic and autophagic HeLa cells per mm^2.

The binding and internalization of RBAc-photosensitized HeLa cells are negatively affected by competing sugars (Table 2).

Macrophage recruitment and FKN release

Macrophages, cultured on the upper chamber of the 8 μm pore-size PET transwell, are actively recruited by photosensitized HeLa cells seeded in the lower chamber (Figure 2a–c). The speed and the extent of macrophages recruitment depend on the dead cell type present in the lower chamber. The highest recruitment was measured for EBSS-starved and PDT-induced autophagic cells. In particular, autophagic EBSS-starved HeLa cells are the most efficient to attract macrophages (Figure 2a and Table 3). It is noteworthy that human macrophages are better recruited than murine ones by dead cells with an efficiency of about 30%.

The different percentage of migrating macrophages was related to the amount of FKN shed by the dead cells (Figure 2d). FKN released into the culture medium was in decreasing order of concentration: autophagic EBSS-starved (52.4 ± 0.53 pg/mL), apoptotic (45.25 ± 0.33 pg/mL) and autophagic PDT-induced (35.7 ± 0.34 pg/mL) HeLa cells. Interestingly, apoptotic PMC-induced or necrotic HS-induced HeLa cells do not secrete this chemokine in the culture medium (Figure 2d). The use of a neutralizing antibody against FKN did not completely block macrophagic migration in our assay.

HSP70 protein

RBAc-PDT induced the plasma membrane translocation and release of HSP70 protein (Figure 2e). Particularly, the increment of translocated HSP70 ranged from about 2- (1 h post-PDT) to 6.5-fold (72 h post-PDT) the untreated value (Figure 2e).

Soluble HSP70 was also measured in the culture medium of PDT-treated HeLa cells during the entire recovery after irradiation, reaching about 4-fold the untreated value at 24 h post-PDT (Figure 2E).

Macrophage production of cytokines

Macrophages secrete anti- and pro-inflammatory cytokines, i.e. TGFβ, IL10 and TNFα, during chemotaxis and phagocytosis assays. Differences in relation to the dead cells type and cell death inducer are observed. Macrophages challenged with photosensitized HeLa cells produce a significant higher amount of anti-inflammatory cytokine TGFβ than those cultured with apoptotic PMC-induced cells. In particular, EBSS-starved and PDT-treated autophagic HeLa cells induce the highest macrophagic release of this cytokine. No difference was observed in IL10 secretion when macrophages are cultured in presence of apoptotic PMC-induced or photokilled HeLa cells, while EBSS-starved autophagic HeLa cells stimulate the highest IL10 secretion (Figure 3a,b,a',b').

Macrophages incubated for 3 h with necrotic HS-induced HeLa cells release the highest levels of TNFα in the culture medium (253 pg/mL). TNFα was also released during macrophages migration towards apoptotic and autophagic PDT-induced and EBSS-starved HeLa cells. TNFα was not detected in the culture medium of macrophages challenged

Table 2 Number of Hepatic Sinusoidal Endothelial (HSE) and Kupffer Cells (KC) of the periportal (pp) and perivenous (pv) region binding (B) and internalizing (I) apoptotic and autophagic HeLa cells per mm^2

	HSE				KC			
	pp		pv		pp		pv	
HeLa cells perfused	**B**	**I**	**B**	**I**	**B**	**I**	**B**	**I**
Viable	2.3 ± 0.09	N.D.	1.5 ± 0.1	N.D.	N.D.	1.1 ± 0.2	N.D.	N.D.
PMC 4h	307.7 ± 13	10.1 ± 1.7	92.8 ± 13	0.7 ± 0.02	61.7 ± 6.5	12.5 ± 3.7	13.7 ± 7.1	1.5 ± 1.7
RBAc-PDT (12h rec)	295.2 ± 11.9	23.21 ± 8.3	114.9 ± 14.9	N.D.	102.4 ± 14.9	19.6 ± 5.9	26.8 ± 3.6	15.5 ± 2.4
RBAc-PDT (8h rec)	242.8 ± 16.7	22.6 ± 1.5	85.1 ± 12.5	N.D.	82.1 ± 17.8	23.8 ± 4.2	21.4 ± 5.9	10.7 ± 1.5
+Competing sugar mixture								
Viable	2.1 ± 0.4	N.D.	0.9 ± 0.1	N.D.	N.D.	N.D.	N.D.	N.D.
PMC 4h	92.31 ± 11.9	3.03 ± 0.2	37.12 ± 3.7	0.2 ± 0.01	18.5 ± 2.7	3.75 ± 0.4	5.48 ± 0.9	0.6 ± 0.01
RBAc-PDT (12h rec)	29.52 ± 8.9	2.3 ± 0.1	22.98 ± 6.1	N.D.	10.24 ± 1.2	1.96 ± 0.02	5.36 ± 0.3	3.1 ± 0.9
RBAc-PDT (8h rec)	24.28 ± 7.2	2.26 ± 0.3	17.02 ± 19	N.D.	8.21 ± 1.1	2.38 ± 0.5	4.28 ± 0.1	2.14 ± 0.4

The average number of hepatic sinusoidal cells binding or internalizing dead HeLa cells was measured after hematoxylin eosin staining of paraffin sections of rat livers injected with apoptotic and autophagic RBAc-PDT induced HeLa cells, by counting 0,168 mm^2 of livers section for each sample.
+Competing sugar mixture: livers perfused with a mixture of Galactose/N-acetylglucosamine/mannose/N-acetylgalactosamine/Fucose (80 mM final concentration) before dead HeLa cells administration.
Viable: untreated HeLa cells; PMC 4 h: apoptotic puromycin (20 μM 4 h)-induced HeLa cells; RBAc-PDT (12h rec): apoptotic PDT-induced HeLa cells, 12 h of recovery post PDT; RBAc-PDT (8 h rec): autophagic PDT-induced HeLa cells, 8 h of recovery post PDT.
N.D. Not Detected value, corresponding to 0 cells counted
RBAc-PDT: HeLa cells incubated with Rose Bengal Acetate for 60 min followed by 90 seconds irradiation with green light (1.6 J/cm^2) and then by recovery in fresh medium (8 and 12 h).
Each value is the average ±SD of three independent experiments.
All values RBAc-PDT are significantly different ($p < 0.05$) with respect to PMC 20 μM 4 h.

with viable and apoptotic PMC-induced HeLa cells (Figure 3c–c′).

In vivo recruitment of macrophages

Inflammation is resolved within three days PI in the rat calf muscles inoculated with pyrogen-free water, the negative control. The number of CD68 positive macrophages infiltrating the site of inoculum with viable HeLa cells or EMEM culture medium is low during 15 days PI and it is not significantly different from the negative control.

A significant increase (4-fold respect to viable HeLa cells and EMEM culture medium, inocula controls) of CD68 positive cells was observed in muscles inoculated with photokilled HeLa cells. Indeed, PDT-induced autophagic cells more efficiently recruit CD68 positive cells to the inoculum site than PDT-induced apoptotic HeLa cells. The number of CD68 positive cells was high at three days PI and progressively decreased during 15 days of observation. Conversely, CD68 positive cells increase during 15 days PI in muscles inoculated with EBSS-starved autophagic HeLa cells or its conditioned medium. In particular, the highest number (5-fold respect to viable HeLa cells and EMEM culture medium) of infiltrating cells is found after 15 days PI in the EBSS-starved autophagic HeLa cells sample. When muscles are inoculated with RBAc-induced autophagic HeLa cells conditioned medium, FKN or latex beads no significant changes are observed (Table 4).

Inocula of apoptotic and autophagic PDT-induced HeLa cells and their conditioned media stimulate the recruitment of fibroblasts and endothelial cells expressing TGFβ RII, as detected by the increased number of TGFβ RII positive cells. This positivity progressively decreased from 3 to 15 days PI. Interestingly, the number of TGFβ RII positive cells increases up to 15 days PI at the site of apoptotic PDT-induced conditioned medium inoculum.

Moreover, the number of TGFβ RII positive cells was significantly higher, of about 1.5-fold at 7 and 15 days PI, in muscles inoculated with apoptotic RBAc-induced HeLa cells conditioned medium compared with RBAc-induced autophagic HeLa cells one (Table 4). Figure 4 shows CD68 and TGFβ RII positive cells infiltrated in rats calf muscles.

Discussion

Phagocytosis represents a critical effector mechanism of the immune system for the disposal of pathogens and aged, damaged or dying cells. Failed or defective clearance has emerged as an important contributing factor to a range of disease processes, such as autoimmune diseases, atherosclerosis and neurological diseases. In cancer, both in the development and progression, the role of dead/dying cells removal is enigmatic since it can have a beneficial and detrimental effect.[23] Moreover, also the role of factors released by phagocytes upon dead cells clearance in triggering immune response in normal and tumour environment is pivotal as well as immunogenic molecules released by dead cells in cancer therapies design.[23]

Also in PDT, the recent studies are primarily addressed to understand the capability to induce immunogenic killing of the tumour cells rather than their removal by phagocytes and the impact of the removal on outcome of the treatment. In addition, the molecular mechanisms participating in the clearance of autophagic cells (no matter of the induction

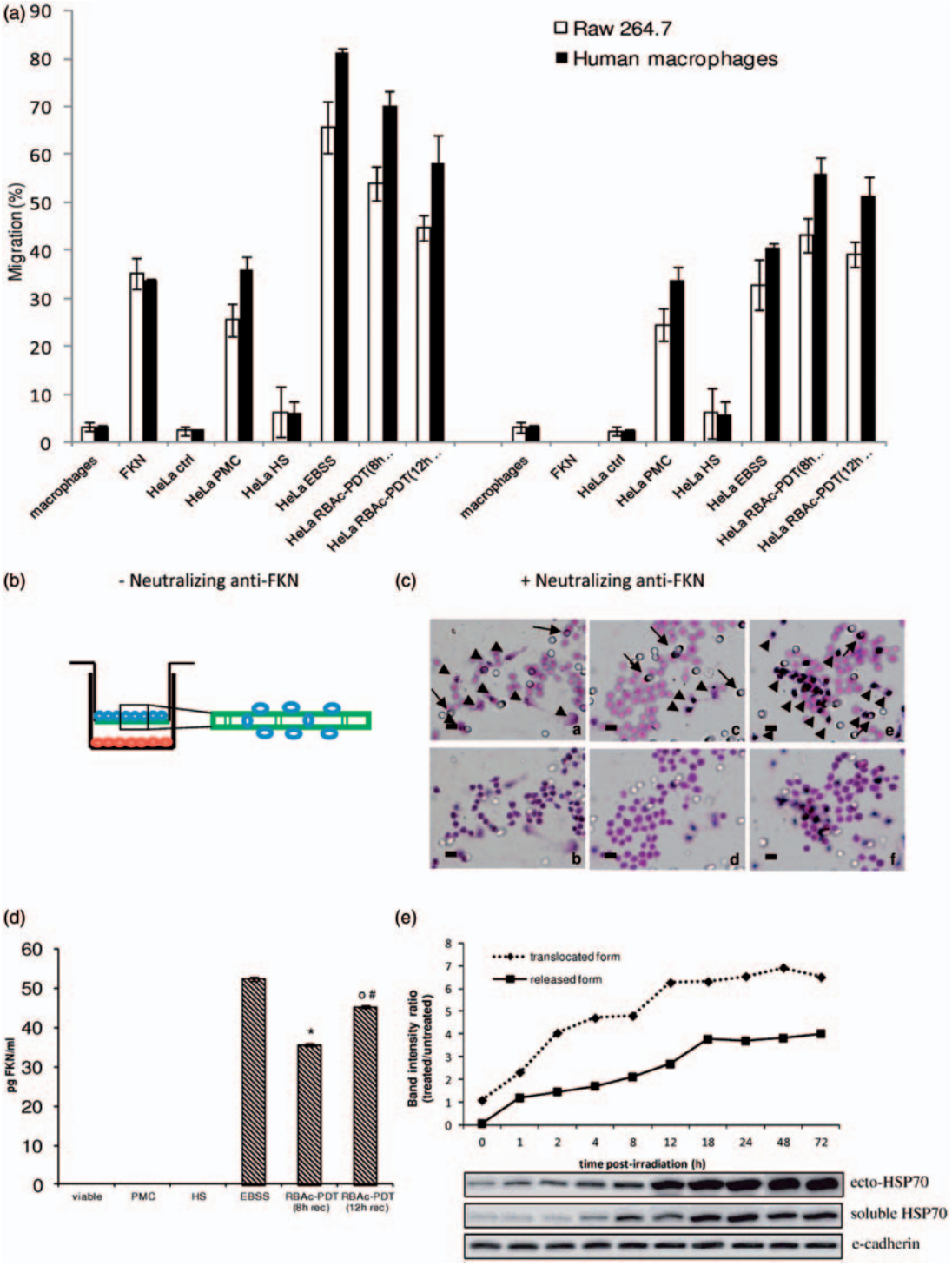

Figure 2 Shedding of HeLa cells fractalkine and recruitment of human and murine macrophages

a: Migration of isolated human and murine Raw 264.7 macrophages towards dead HeLa cells. The values represent the percentage of the total macrophage migration, i.e. macrophages localized on the upper surface, in the pores and on the lower surface of a 8 μm pore-size transwell in the presence (+) or in the absence (−) of anti-FKN Ab and are the mean + SD of three independent experiments. The total number of macrophages was taken as 100%

Macrophages were seeded in the upper chamber of the transwell while in the lower chamber were incubated dead HeLa cells as reported below. All the counts refer to 3 h of culture

Macrophages: macrophages cultured in complete DMEM; FKN: macrophages incubated with 60 pg/mL recombinant murine fractalkine; HeLa viable: macrophages co-cultured with viable HeLa cells; HeLa PMC: macrophages co-cultured with apoptotic PMC (20 μmol/L 4 h)-induced HeLa cells; HeLa HS: macrophages co-cultured with necrotic heat shock (48–50°C 1 h)-induced HeLa cells; HeLa EBSS: macrophages co-cultured with autophagic starvation (EBSS 6 h)-induced HeLa cells; HeLa RBAc-PDT (8 h rec): macrophages co-cultured with autophagic PDT-induced HeLa cells, 8 h of recovery post PDT; HeLa RBAc-PDT (12 h rec): macrophages co-cultured with apoptotic PDT-induced HeLa cells, 12 h of recovery post PDT

RBAc-PDT: HeLa cells incubated with rose bengal acetate for 60 min followed by 90 s irradiation with green light (1.6 J/cm^2) and then by recovery in fresh *medium* (8 and 12 h). (A color version of this figure is available in the online journal)

*Values significantly different ($P < 0.05$) with respect to the macrophages, FKN, HeLa viable, HeLa PMC and HeLa HS values; °values significantly different ($P < 0.05$) with respect to the HeLa EBSS values; #values significantly different ($P < 0.05$) with respect to the HeLa RBAc-PDT (8 h rec) values; §values significantly different ($P < 0.05$) with respect to the correspondent (−anti-FKN Ab) values

b: Schematic diagram of a 8 μm pore-size transwell

c: Light microscope micrographs of haematoxylin–eosin stained human macrophages localized on the lower (a, c, e) and in the upper (b, d, f) surface of a 8 μm pore-size transwell. (a,b) Human macrophages co-cultured with autophagic RBAc-PDT-induced HeLa cells, 8 h of recovery post PDT; (c,d) human macrophages co-cultured with apoptotic RBAc-PDT-induced HeLa cells, 12 h of recovery; (e,f) human macrophages co-cultured with autophagic starvation (EBSS 6 h)-induced HeLa cells. Arrows show macrophages localized in the pores; arrows heads show macrophages attached on the lower surface of porous membrane. Bars = 10 μm

d: ELISA assay of FKN release by dead HeLa cells. The values, reported as pg/mL, are the mean ± SD of three independent experiments. viable: HeLa cells cultured in complete EMEM; PMC: apoptotic PMC (20 μmol/L, 4 h)-induced HeLa cells; HS: necrotic heat shock (48–50°C, 1 h)-induced HeLa cells; EBSS: autophagic starvation (EBSS 6 h)-induced HeLa cells; RBAc-PDT (8 h rec): autophagic RBAc-PDT-induced HeLa cells; 8 h of recovery post PDT; RBAc-PDT (12 h rec): apoptotic RBAc-PDT-induced HeLa cells, 12 h of recovery post PDT; RBAc-PDT: HeLa cells incubated with rose bengal acetate for 60 min followed by 90 s irradiation with green light (1.6 J/cm^2) and then by recovery in fresh medium (8 and 12 h)

*Values significantly different ($P < 0.05$) with respect to the EBSS values; °values significantly different ($P < 0.05$) with respect to the PMC values; #values significantly different ($P < 0.05$) between autophagic and apoptotic photosensitized values

e: Kinetic of HSP70 membrane translocation (ecto-HSP70) and release (soluble HSP70). SDS-PAGE was performed on the supernatants and membrane fraction (30 μg protein/lane) of HeLa cells subjected to RBAc-PDT (10^{-5} mol/L RBAc, 1 h, 1.6 J/cm^2, 90 s) at the indicated time intervals and electroblotted to nitrocellulose membrane. Western blot was developed with monoclonal antibody against HSP70 (70 kDa). The amount of HSP70 protein was reported as band intensity ratio (treated/untreated) measured by densitometer analysis. E-cadherin expression is shown as a control. Actin is absent in the membrane protein fraction. The data are the mean ± SD of three independent experiments

(A color version of this figure is available in the online journal)

Table 3 Percentage of Human (H) and Murine Raw 264.7 (M) macrophages migrating towards HeLa cells after 3h of co-culture in 8 Lim pore size PET transwells

HeLa cells seeded in the lower chamber	Percentage of macrophages					
	8 Lim pore size PET					
	Upper surface		Pores		Lower surface	
	M	H	M	H	M	H
−anti-FKN Ab						
DMEM	96,7 ± 4,8	95,3 ± 4,3	3,3 ± 0,4	4,7 ± 0,2	N.D.	N.D.
FKN	65.1 ± 2,4	61,84 ± 2,8	11,5 ± 1,2	12,07 ± 1,1	23,4 ± 1,1	26,09 ± 2,1
viable	97,6 ± 3,1	97,4 ± 4,2	2,4 ± 0,4	2,6 ± 0,2	N.D.	N.D.
PMC 4h	74,5 ± 3,5*	62,68 ± 5,2	17,6 ± 2,8*	26,4 ± 3,1*	7,8 ± 0,4*	10,92 ± 0,9*
HS 1h	93,6 ± 6,7*	94,24 ± 7,1*	4,7 ± 0,3*	4,23 ± 0,2*	1,7 ± 0,05*	1,53 ± 0,01*
EBSS 6h	34,2 ± 4,5*	17,88 ± 2,9*	27,4 ± 3,9*	34,25 ± 4,2*	38,3 ± 3,3*	47,87 ± 4,1*
RBAc-PDT (8h rec)	46,1 ± 2,5*°	29,93 ± 3,2*°	27,5 ± 2,3*°	35,75 ± 4,9*	26,4 ± 2,5*°	34,32 ± 3,9*°
RBAc-PDT (12h rec)	55,2 ± 2,2*#	41,76 ± 3,8*#	24,8 ± 2,3*#	32,24 ± 4,1*#	20 ± 3*#	26 ± 3,1#
+ anti-FKN Ab						
DMEM	95,7 ± 4,5	94,3 ± 4,1	4,3 ± 0,4	5,7 ± 0,2	N.D.	N.D.
FKN	95,3 ± 3,9	93,9 ± 4,2	4,7 ± 0,1	6,1 ± 0,9	N.D.	N.D.
viable	97,72 ± 4,1	97,53 ± 3,9	2,28 ± 0,2	2,47 ± 0,3	N.D.	N.D.
PMC 4h	75,62 ± 3,3	64,18 ± 2,5	16,89 ± 2,5	25,34 ± 3,6	7,49 ± 1,1	10,48 ± 0,8
HS 1h	93,79 ± 7,1	94,47 ± 6,5	4,56 ± 0,2	4,06 ± 0,1	1,65 ± 0,02	1,47 ± 0,03
EBSS 6h	67,15 ± 3,1	58,95 ± 3,5	13,7 ± 1,1	17,12 ± 0,9	19,15 ± 1,5	23,93 ± 2,1
RBAc-PDT (8h rec)	56,88 ± 3,2°	43,94 ± 2,3°	22 ± 0,9°	28,6 ± 1,2°	21,12 ± 2,1	27,46 ± 2,9°
RBAc-PDT (12h rec)	60,58 ± 2,9#	48,75 ± 2,1#	21,82 ± 0,2#	28,37 ± 1,1	17,6 ± 2,7#	22,88 ± 2,3#

DMEM: Dulbecco's Modified Eagle Medium (DMEM) supplemented with 10% Foetal Bovine Serum, 2 mM L-glutamine, 100 IU/ml penicillin and streptomycin solution and 10000 U/ml amphotericin B; FKN: 60 pg/ml recombinant murine fractalkine; viable: untreated HeLa cells; PMC 4h: apoptotic puromycin (20 liM 4h)-induced HeLa cells; HS 1h: necrotic heat shock (48-50°C 1h)-induced HeLa cells; EBSS 6h: autophagic starvation (EBSS 6h)-induced HeLa cells; RBAc-PDT (8h rec): autophagic PDT-induced HeLa cells, 8 h of recovery post PDT; RBAc-PDT (12h rec): apoptotic PDT-induced HeLa cells, 12 h of recovery post PDT.

RBAc-PDT: HeLa cells incubated with Rose Bengal Acetate for 60 min followed by 90 seconds irradiation with green light (1.6 J/cm^2) and then by recovery in fresh medium (8 and 12 h). N.D. Not Detected value, corresponding to 0 cells counted

Values are the mean ± SD of three independent experiments. At least 500 cells were scored for each sample.

*values significantly different ($p < 0,05$) with respect to FKN

°values significantly different ($p < 0,05$) with respect to EBSS

#values significantly different ($p < 0,05$) with respect to PMC

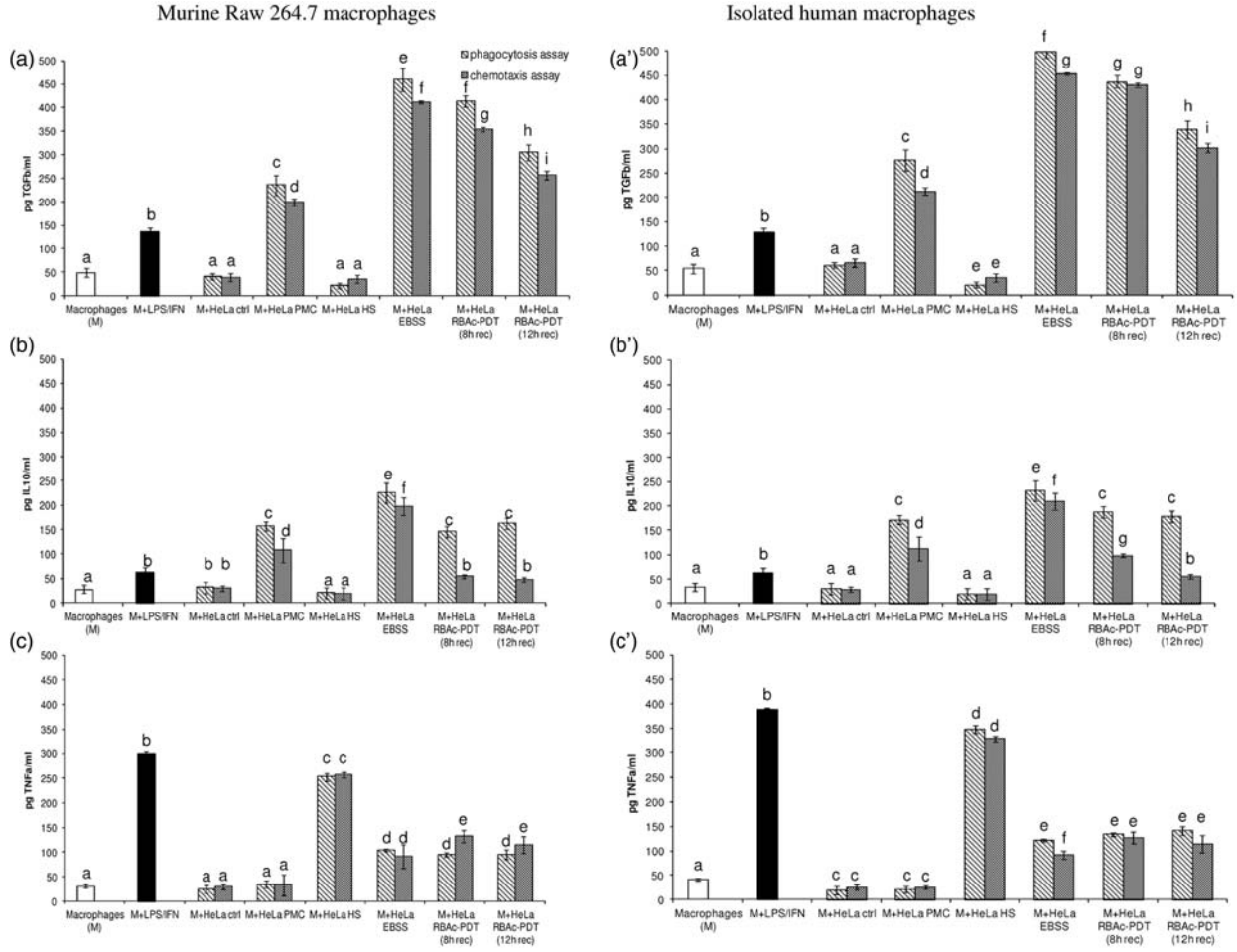

Figure 3 Pro- and anti-inflammatory cytokines released by human and murine macrophages

ELISA assays of TGFβ (a–a'), IL-10 (b–b') and TNFα (c–c') released by isolated human and murine Raw 264.7 macrophages during *in vitro* phagocytosis and chemotaxis experiments. The values, reported as pg/mL, are the mean ± SD of three independent experiments. Macrophages (M): macrophages cultured in complete DMEM; M + LPS/IFNγ: macrophages stimulated 24 h with LPS (1 mg/mL) and IFNγ (100 UI/mL); M + HeLa ctrl: macrophages cultured 3 h in the presence of untreated HeLa cells; M + HeLa PMC: macrophages cultured 3 h in the presence of apoptotic PMC (20 μmol/L 4 h)-induced HeLa cells; M + HeLa HS: macrophages cultured 3 h in the presence of necrotic heat shock (48–50°C 1 h)-induced HeLa cells; M + HeLa EBSS: macrophages cultured 3 h in the presence of autophagic starvation (EBSS 6 h)-induced HeLa cells; M + HeLa RBAc-PDT (8 h rec): macrophages cultured 3 h in the presence of autophagic PDT-induced HeLa cells at 8 h of recovery post PDT; M + HeLa RBAc-PDT (12 h rec): macrophages cultured 3 h in the presence of apoptotic PDT-induced HeLa cells at 12 h of recovery post PDT

RBAc-PDT: HeLa cells incubated with rose bengal acetate for 60 min followed by 90 s irradiation with green light (1.6 J/cm^2) and then by recovery in fresh medium (8 and 12 h)

Results that are significantly different ($P < 0.05$) between the samples are indicated by different characters above the columns

signal) are less well known than those implicated in the removal of apoptotic ones.[24,25] In this context, our results represent the first comparison of the removal of autophagic and apoptotic photokilled cells and provide more information on the still poorly explored field of the removal of autophagic cells.

In this report, we provided *in vitro* and *in vivo* evidence of the efficient clearance of RBAc-photokilled HeLa cells, in terms of recruitment, recognition and removal. Since RBAc-PDT induces a prolonged cytotoxicity and a time-related and independent cell death by apoptosis and autophagy in HeLa cells,[21] here we describe the clearance of RBAc-photosensitized autophagic and apoptotic cells. The study has been performed in two kinds of paradigm: (1) clearance of HeLa cells killed by autophagy and apoptosis triggered following a precise timing upon the same treatment, i.e. RBAc-PDT; (2) clearance of autophagic and apoptotic HeLa cells generated by specific different inducers, i.e. EBSS, RBAc-PDT and PMC.

In our hands, the efficiency of the recognition of dead cells is related to the type of death, i.e. apoptotic and autophagic, and, within the same type of dead cells, to the specific inducer. In fact, apoptotic PDT-generated HeLa cells are preferred 'food' to photosensitized autophagic cells; and photokilled cells are more efficiently recognized by murine and human macrophages than HeLa cells dying by EBSS-starvation, HS or PMC. Our data agree with Zhou *et al.*'s[26] findings showing the internalization of apoptotic photofrin-PDT-induced murine mammary tumour C127 cells by Raw 264.7 macrophages. Recently, it has also been demonstrated that murine colon carcinoma CT26 cells exposed to hypericin (Hyp)-PDT were engulfed

Table 4 Number of macrophages recruited by dying HeLa cells per mm^2 of calf muscles

HeLa cells inoculated into calf rat muscles	CD 68			TGFβ RII		
	post-inoculation days			post-inoculation days		
	3	7	15	3	7	15
Viable	185.2 ± 23.8	132.3 ± 8.5	129.5 ± 13.2	171.9 ± 12.3	148.1 ± 21.1	132.3 ± 11.5
EMEM	158.7 ± 10.6	81.6 ± 15.9	79.4 ± 13.2	116.4 ± 23	125.4 ± 16.1	120.1 ± 19.12
Latex	214.3 ± 11.9	208.9 ± 20.1	198.4 ± 18.3	ND	ND	ND
FKN	341.3 ± 33.1	357.1 ± 23.5	367.7 ± 35.8	ND	ND	ND
PMC 4 h	396.8 ± 5.3	264.5 ± 17.2	185.2 ± 18.5	182.5 ± 20.7	187.8 ± 13.4	201.5 ± 9.5
HS 1 h	397.1 ± 2.6	268.6 ± 23.5	183.9 ± 13.2	230.1 ± 11.1	195.8 ± 15.3	220.9 ± 10.9
EBSS 6 h	357.7 ± 25.6	500 ± 17.8	547.6 ± 21.2	ND	ND	ND
CM (EBSS 6 h)	195.8 ± 11.7	269.8 ± 9.1	343.9 ± 7.9	ND	ND	ND
RBAc-PDT (8 h rec)	608.5 ± 7.9	529.1 ± 5.8	423.3 ± 5.5	345.7 ± 21.5	317.5 ± 23	306.9 ± 12.5
CM (RBAc-PDT 8 h rec)	435.6 ± 14.9*	432.4 ± 11.9*	476.2 ± 5.5*	375.7 ± 21.4*	257.9 ± 20.1*	198.4 ± 12.3*
RBAc-PDT (12 h rec)	502.6 ± 15.9	495.1 ± 20.1	396.8 ± 9.1	248.7 ± 11.6	306.9 ± 15.1	280.4 ± 12.2
CM (RBAc-PDT 12 h rec)	449.7 ± 10.6°	264.5 ± 7.9°	370.4 ± 6.3°	343.9 ± 15.2°	321.5 ± 12.5°	362.4 ± 17.1°

Viable: muscles inoculated with untreated HeLa cells; EMEM: muscles inoculated with EMEM (10% FCS); latex: muscles inoculated with 5×10^5 latex beads; FKN: muscles inoculated with 6 pg of fractalkine; PMC 4 h: muscles inoculated with apoptotic PMC (20 μmol/L 4 h)-induced HeLa cells; HS 1 h: muscles inoculated with necrotic heat shock (48–50°C 1 h)-induced HeLa cells; EBSS 6 h: muscles inoculated with autophagic starvation (EBSS 6 h)-induced HeLa cells; CM (EBSS 6 h): muscles inoculated with conditioned medium of autophagic starvation (EBSS 6 h)-induced HeLa cells; RBAc-PDT (8 h rec): muscles inoculated with autophagic PDT-induced HeLa cells, 8 h of recovery post PDT; HeLa RBAc-PDT (12 h rec): muscles inoculated with apoptotic PDT-induced apoptotic HeLa cells; 12 h of recovery post PDT; CM (RBAc-PDT 8 h rec): muscles inoculated with conditioned medium of autophagic PDT-induced HeLa cells, 8 h of recovery post PDT; CM (RBAc-PDT 12 h rec): muscles inoculated with conditioned medium of apoptotic PDT-induced HeLa cells; 12 h of recovery post PDT; RBAc-PDT: HeLa cells incubated with rose bengal acetate for 60 min followed by 90 s irradiation with green light (1.6 J/cm^2) and then by recovery in fresh medium (8 and 12 h); ND: not done.
The average number of macrophages recruited in Wistar rat calf muscles inoculated with dying HeLa cells was measured after immunohistochemical analysis of cells expressing the CD68 antigen and type II of TGFβ receptor. Values are the average ± SD of three independent experiments.
*Values significantly different ($P < 0.05$) with respect to RBAc-PDT (8 h rec).
°Values significantly different ($P < 0.05$) with respect to RBAc-PDT (12 h rec).

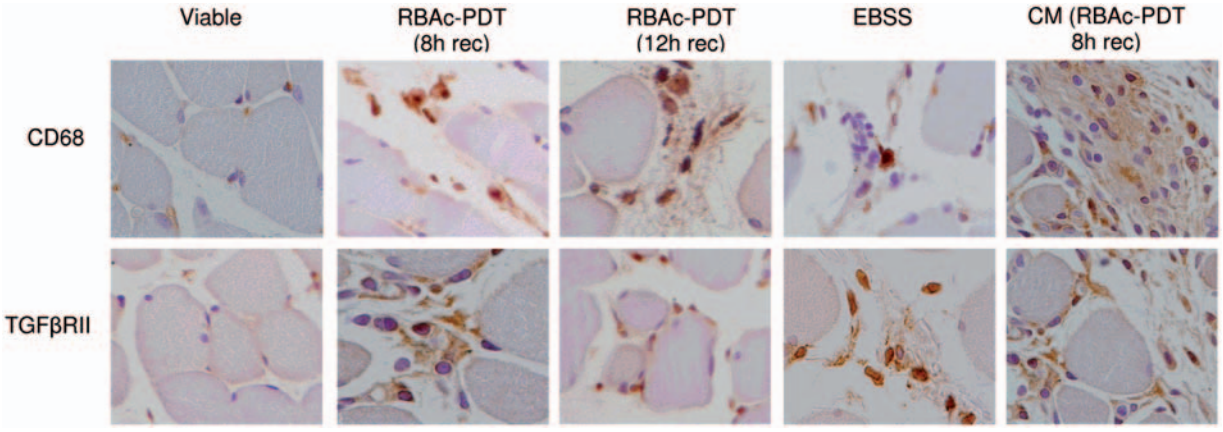

Figure 4 Recruitment of macrophages and activated fibroblasts and endothelial cells *in vivo*.
Light microscope micrographs of anti-CD68 and anti-TGFβRII positive cells infiltrated in rat calf muscles inoculated with dying HeLa cells.
Viable: muscles inoculated with untreated HeLa cells; RBAc-PDT (8 h rec): muscles inoculated with autophagic PDT-induced HeLa cells; RBAc-PDT (12 h rec): muscles inoculated with apoptotic PDT-induced HeLa cells; EBSS: muscles inoculated with autophagic starvation (EBSS 6 h)-induced HeLa cells; CM (RBAc-PDT 8 h rec): muscles inoculated with conditioned medium of autophagic PDT-induced HeLa cells. RBAc-PDT: HeLa cells incubated with rose bengal acetate for 60 min followed by 90 s irradiation with green light (1.6 J/cm^2) and then by recovery in fresh medium (8 and 12 h). Original magnification × 60. (A color version of this figure is available in the online journal)

by murine JAWSII DCs; similarly, human bladder carcinoma T24 cells were phagocytosed by murine Mf4/4 macrophages and human DCs.[27,28]

For the efficient removal of dead cells, a network of interactions has been evolved between the dying cells and the phagocytes. In particular, the recognition and subsequent removal of the apoptotic cells depend on specific molecules exposed on the plasma membrane of dead cells, named 'eat me' signals. In fact, dying apoptotic cells expose a lot of 'eat me' molecules specifically recognized by several receptors

on phagocytes.[29] One of the best characterized 'eat me' signals is the phosphatidylserine (PtdSer) externalized on dead cells plasma membrane,[30] but changes in carbohydrate residues of glycoproteins,[31] calreticulin[32] and the exposure of DNA[33] on dying cells have been also proposed as signal molecules. Moreover, the analysis of the specific cell surface changes on autophagic cells is still in its infancy. Petrovski *et al*. showed that the uptake of human breast cancer MCF7 autophagic cells by non-professional MCF7 and human isolated macrophages is not inhibited by recombinant annexin-V, indicating that PtdSer-independent cell surface changes are induced in cells dying through autophagy.[25]

To date, very little is known of the cell surface changes occurring on photosensitized dead cells that would make them edible for phagocytes. Merchant *et al*. suggest a possible role for SAP, CRP, PTX3 and ficolin 1 proteins in clearance of tumoural-photokilled cells.[34,35] In fact, they demonstrate that PDT treatment by photofrin, 5-Aminolevulinic acid (ALA), Benzoporfirin derivative (BPD) and m-tetra hydroxy phenyl chlorin (mTHPC) increases in Lewis lung carcinomas (LLC) the expression of *SAP* gene,[34] whose product facilitates the disposal of dead cells by professional phagocytes.[36] In addition, Merchant demonstrates that also in C57BL/6 mice bearing LLC tumour photofrin-PDT upregulates *SAP* gene expression. The authors shown that SAP remains localized to the cells suggesting that the protein could act as molecule attracting phagocytes.[34] Moreover, photofrin-PDT also induces upregulation of CRP, PTX3 and ficolin 1 in LLC and A549 cells.[35] Since these proteins are specialized in facilitating the removal of dying cells,[36,37] the authors suggest a possible role in phagocytosis of photodynamically treated cells.[35]

We have already reported exposure of PtdSer on the surface of autophagic and apoptotic RBAc photosensitized HeLa cells in our previous works.[18,20] Here, we describe the changes in cell surface glycans (amount and distribution) induced by RBAc-PDT on both apoptotic and autophagic HeLa cells and suggest the role of sugars in recognition during macrophagic phagocytosis.

RBAc-induced glycans rearrangement, dependent on cell death type and, within the same type of death, on the death inducer, influences the clearance mechanism *in vitro* and *in vivo*. Accordingly, literature data report that sugar residues, upon interaction with specific hepatic lectin-like receptors, ensure the rapid and efficient clearance of apoptotic cells performed by liver sinusoidal cells. The amount of dead cells removed via carbohydrate receptors depends on the number of binding sites exposed on sinusoidal cells surface.[31,38]

In this context, our results demonstrate that the majority of dead cells are bound by HSEs and KCs of the pp region rather than pv region, in agreement with Dini and Carlà[39] reporting that the cells of the pp tract express double amount of carbohydrate specific receptors than pv cells.

Efficient tethering and engulfment of apoptotic cells require that the phagocytes effectively and efficiently migrate to the sites of dead cells. For this purpose, dead cells release chemoattractant molecules ('find me' signals) soon after the engagement of the cell death program.[40] Indeed, the initial step of the clearance mechanism is the attraction of phagocytes to the site of apoptotic cells. Several mechanisms involving molecules such as S19,[41] endothelial monocyte-activating polypeptide II,[42] Lysophosphatidylcholine (LPC),[43] adenosine triphosphate[44] and FKN[45] have been proposed to play a role for the attraction of phagocytes to apoptotic cells. Conversely, only the release of the 'find me' signal LPC has been attributed to dead autophagic cells.[46] The present work demonstrates the involvement of a further 'sensing' mechanism, based on release of the FKN, a chemokine and adhesion molecule CX3CL1, attracting scavengers cells to autophagic dead cells. Both autophagic and apoptotic RBAc-PDT-generated HeLa cells release FKN. Particularly, photokilled apoptotic cells are better 'producers' of FKN than autophagic cells. Our findings also suggest that the cell death type and the inducer are pivotal for the release of FKN. In fact, PMC and HS do not induce FKN secretion, while EBSS-starvation is very efficient at inducing FKN release. FKN released by photosensitized dead cells contributes to macrophage movement. Indeed, the use of a neutralizing antibody against FKN decreases macrophages migration towards dead cells. The efficient cell migration induced by RBAc-PDT-treated cells suggests the pivotal involvement of FKN in recruiting macrophages, but the fact that additional factors released by dead cells could result chemoattractant for macrophages cannot be excluded. These are recruited in decreasing order by autophagic EBSS-starved, photosensitized autophagic HeLa cells, apoptotic PDT-generated and apoptotic PMC-induced cells.

The *in vivo* analysis also gives evidence of the efficiency of macrophage recruitment by the photokilled cells and strongly confirms the role of the soluble factors released by the apoptotic and autophagic RBAc-PDT generated HeLa cells. Interestingly, the response (in terms of recruitment of fibroblasts and endothelial cells) evoked by the inoculum conditioned medium of apoptotic RBAc-PDT induced HeLa cells alone, is much stronger than the response observed when apoptotic photokilled HeLa cells are inoculated. This is probably due to a longer permanence of soluble signals into the muscle with respect to the dead cells that are quickly removed by the macrophages, thus getting rid of the 'cytokine factory'.

Dying tumour cells are a rich source of antigens whose immunomodulatory effects are currently debated. Several studies suggest that molecules, called alarmins or DAMPs, normally retained within viable cells are crucially involved in immunogenic apoptosis when exposed on dead cell surface or released. In fact, the idea that apoptosis is an immunological silent or even tolerogenic cell death type has been recently invalidated since in certain conditions apoptosis can induce significant immunological responses due to the release of danger molecules alerting the immune system.[14]

Among cancer therapies, PDT effectively generates several DAMPs.[47] Moreover, if the association of DAMPs to PDT-induced apoptosis has been investigated, knowledge is scarce about the DAMPs associated in PDT-induced autophagic cell death. The best characterized DAMPs involved in PDT-triggered apoptosis are HSPs, especially HSP70, as described for squamous cells carcinoma SCCVII,[48] murine mammary tumour cells C127,[49] HeLa, human lung adenocarcinoma cells ASTC-a-1[26] during

photofrin-PDT and human bladder carcinoma T24 cells during Hyp-PDT.[28]

Our data show the dynamic translocation (ecto-HSP70) and the secretion of HSP70 not only in apoptotic RBAc-photokilled HeLa cells but also in autophagic cells.

Ecto-HSP70 plays an important role in the opsonization of cancer cells[50] that could serve to activate the immune effectors and provide a specific signal for macrophages to produce pro-inflammatory cytokines.

We speculate that also in RBAc-PDT, ecto-HSP70 acts as a 'danger signal' alerting the host immune system. In fact, in our *in vivo* experiments we observe that photokilled HeLa cells not only recruit macrophages, as reported above, but also recruit activated fibroblasts and endothelial cells. Moreover, macrophages challenged with RBAc photosensitized HeLa cells produce a discrete amount of TNFα, a pro-inflammatory cytokine. This is in line with similar results obtained by using Raw 264.7 and mouse peritoneal macrophages incubated with photofrin-treated C127 cells.[26,49] The amount of pro-inflammatory cytokines produced by macrophages when challenged with EBSS-starved and autophagic RBAc-PDT induced HeLa cells is not as massive as reported for autophagic tamoxifen-induced MCF-7 cells, which stimulate the monocytes-derived human macrophages to produce pro-inflammatory cytokines IL6, TNFα, IL12B and IL23B.[25]

Our results reveal that macrophages produce a relevant amount of TGFβ, a well-known immunomodulatory cytokine,[51–53] and low level of IL-10, an immunosuppressive cytokine,[54–56] when challenged with photokilled HeLa cells, suggesting that tumour cells killed by RBAc-PDT can elicit a positive immunomodulatory response.

In fact, several papers outline that in cancer diseases the TGFβ and IL-10 biological activities are highly context-dependent.[57–61] In particular, TGFβ depending on tumour stages can exert a dual and opposite effect, i.e. tumour suppression and tumour progression. TGFβ suppresses premalignant progression, inhibits cell cycle, triggers apoptotic cell death, modulates cell invasion, and immune cells recruitment and activity and leads to tumour growth, invasion and immune evasion.[57] On the other hand, IL-10 can subvert tumour immune suppression,[58] promote tumour immunity, reduce tumour rejection and growth in mice.[59–61]

In summary, we provide *in vitro* and *in vivo* evidence of the efficient disposal of RBAc-photokilled HeLa cells. This work demonstrates that FKN, released by autophagic and apoptotic RBAc-induced HeLa cells, plays an important role in the attraction of macrophages. The release of TNFα and TGFβ and the parallel low secretion of IL-10 by macrophages following phagocytosis, along with the change in the localization pattern of HSP70 could provide a premise that RBAc-PDT can also elicit immunomodulatory effects.

AUTHORS CONTRIBUTION

All authors participated in the design, interpretation of the studies and analysis of the data and review of the manuscript; LD, EP, BT and VI conducted the experiments, LD wrote the manuscript.

ACKNOWLEDGEMENTS

The work was funded by a grant FUR from the University of Salento to LD.

REFERENCES

1. Castano AP, Demidova TN, Hamblin MR. Mechanism in photodynamic therapy: Part one-Photosensitizer, photochemistry and cellular localization. *Photodiagn Photodyn Ther* 2004;**1**:279–93
2. Plaetzer K, Krammer B, Berlanda J, Berr F, Kiesslich T. Photophysics and photochemistry of photodynamic therapy: fundamental aspects. *Lasers Med Sci* 2009;**24**:259–68
3. Mroz P, Yaroslavsky A, Kharkwal GB, Hamblin MR. Cell death pathways in photodynamic therapy of cancer. *Cancers* 2011;**3**:2516–39
4. Agostinis P, Berg K, Cengel KA, Foster TH, Girotti AW, Gollnick SO, Hahn SM, Hamblin MR, Juzeniene A, Kessel D, Korbelik M, Moan J, Mroz P, Nowis D, Piette J, Wilson BC, Golab J. Photodynamic therapy of cancer: an update. *CA Cancer J Clin* 2011;**61**:250–81
5. Pizova K, Tomankova K, Daskova A, Binder S, Bajgar R, Kolarova H. Photodynamic therapy for enhancing antitumour immunity. *Biomed Pap Med Fac Univ Palacky Olomouc Czech Repub* 2012;**156**:93–102
6. Munoz LE, van Bavel C, Franz S, Berden J, Herrmann M, van der Vlag J. Apoptosis in the pathogenesis of systemic lupus erythematosus. *Lupus* 2008;**17**:371–5
7. Sabroe I, Whyte MK. Incapacitating the immune system in cystic fibrosis. *Nat Med* 2007;**13**:1417–8
8. Hodge S, Hodge G, Scicchitano R, Reynolds PN, Holmes M. Alveolar macrophages from subjects with chronic obstructive pulmonary disease are deficient in their ability to phagocytose apoptotic airway epithelial cells. *Immun Cell Biol* 2003;**81**:289–96
9. Dini L, Vergallo C. Environmental factors affecting phagocytosis of dying cells: smoking and static magnetic fields. In: Kryskop DV, Vandenabeele P (eds). *Phagocytosis of Dying cells: From Molecular Mechanisms to Human Diseases*. Frankfurt: Springer, 2009:409–38
10. de Visser KE, Eichten A, Coussens LM. Paradoxical roles of the immune system during cancer development. *Nat Rev Cancer* 2006;**6**: 24–37
11. Erwig LP, Henson PM. Clearance of apoptotic cells by phagocytes. *Cell Death Diff* 2008;**15**:243–50
12. Grimsley C, Ravichandran KS. Cues for apoptotic cell engulfment: eat-me, don't eat-me and come-get-me signals. *Trends Cell Biol* 2003;**13**:648–56
13. Segal NH, Parsons DW, Peggs KS, Velculescu V, Kinzler KW, Vogelstein B, Allison JP. Epitope landscape in breast and colorectal cancer. *Cancer Res* 2008;**68**:889–92
14. Zitvogel L, Kepp O, Kroemer G. Decoding cell death signals in inflammation and immunity. *Cell* 2010;**140**:798–804
15. Obeid M, Tesniere A, Ghiringhelli F, Fimia GM, Apetoh L, Perfettini JL, Castedo M, Mignot G, Panaretakis T, Casares N, Métivier D, Larochette N, van Endert P, Ciccosanti F, Piacentini M, Zitvogel L, Kroemer G. Calreticulin exposure dictates the immunogenicity of cancer cell death. *Nat Med* 2007;**13**:54–61
16. Májai G, Petrovski G, Fésüs L. Inflammation and the apopto-phagocytic system. *Immunol Lett* 2006;**104**:94–101
17. Panzarini E, Tenuzzo B, Palazzo F, Chionna A, Dini L. Apoptosis induction and mitochondria alteration in human HeLa tumor cells by photoproducts of Rose Bengal acetate. *J Photochem Photobiol B* 2006;**83**:39–47
18. Panzarini E, Tenuzzo B, Dini L. Photodynamic therapy-induced apoptosis of HeLa cells. *Ann NY Acad Sci* 2009;**1171**:617–26
19. Panzarini E, Inguscio V, Dini L. Timing the multiple cell death pathways initiated by Rose Bengal acetate photodynamic therapy. *Cell Death Dis* 2011;**2**:e169
20. Dini L, Inguscio V, Tenuzzo B, Panzarini E. Rose Bengal acetate photodynamic therapy-induced autophagy. *Cancer Biol Ther* 2010;**10**:1048–55

21. Panzarini E, Inguscio V, Dini L. Overview of cell death mechanisms induced by rose bengal acetate-photodynamic therapy. *Int J Photoenergy* 2011;**ID 713726**:11
22. Dini L, Lentini A, Diez Diez G, Rocha M, Falasca L, Serafino L, Vidal-Vanaclocha F. Phagocytosis of apoptotic bodies by liver endothelial cells. *J Cell Sci* 1995;**108**:967–73
23. Elliott MR, Ravichandran KS. Clearance of apoptotic cells: implications in health and disease. *J Cell Biol* 2010;**189**:1059–70
24. Krieser RJ, White K. Engulfment mechanism of apoptotic cells. *Curr Opin Cell Biol* 2002;**14**:734–8
25. Petrovski G, Zahuczky G, Katona K, Vereb G, Martinet W, Nemes Z, Bursch W, Fesus L. Clearance of dying autophagic cells of different origin by professional and non-professional phagocytes. *Cell Death Diff* 2007;**14**:1117–28
26. Zhou F, Xing D, Chen WA. Regulation of HSP70 on activating macrophages using PDT induced apoptotic cells. *Int J Cancer* 2009;**125**:1380–9
27. Garg AD, Krysko DV, Verfaillie T, Kaczmarek A, Ferreira GB, Marysael T, Rubio N, Firczuk M, Mathieu C, Roebroek AJ, Annaert W, Golab JP, Vandenabeele P, Agostinis P. A novel pathway combining calreticulin exposure and ATP secretion in immunogenic cancer cell death. *EMBO J* 2012;**31**:1062–79
28. Garg AD, Krysko DV, Vandenabeele P, Agostinis P. Hypericin-based photodynamic therapy induces surface exposure of damage-associated molecular patterns like HSP70 and calreticulin. *Cancer Immunol Immunother* 2012;**61**:215–21
29. Ravichandran KS, Lorenz U. Engulfment of apoptotic cells: signals for a good meal. *Nature Rev Immunol* 2007;**7**:964–74
30. Balasubramanian K, Schroit AJ. Aminophospholipid asymmetry: a matter of life and death. *Annu Rev Physiol* 2003;**65**:701–34
31. Dini L. Recognizing death: liver phagocytosis of apoptotic cells. *Eur J Histochem* 2000;**44**:217–27
32. Gardai SJ, McPhillips KA, Frasch SC, Janssen WJ, Starefeldt A, Murphy-Ullrich JE. Cell-surface calreticulin initiates clearance of viable or apoptotic cells through trans-activation of LRP on the phagocyte. *Cell* 2005;**123**:321–34
33. Palaniyar N, Nadesalingam J, Clark H, Shih MJ, Dodds AW, Reid KB. Nucleic acid is a novel ligand for innate, immune pattern recognition collectins surfactant proteins A and D and mannose-binding lectin. *J Biol Chem* 2004;**279**:32728–36
34. Merchant S, Sun J, Korbelik M. Dying cells program their expedient disposal: serum amyloid P component upregulation in vivo and in vitro induced by photodynamic therapy of cancer. *Photochem Photobiol Sci* 2007;**6**:1284–9
35. Merchant S, Korbelik M. Upregulation of genes for C-reactive protein and related pentraxin/complement proteins in photodynamic therapy-treated human tumor cells: Enrolment of PI3K/Akt and AP-1. *Immunobiology* 2012;**pii**: S0171–2985(12)00520-7
36. Bijl M, Horst G, Bijzet J, Bootsma H, Limburg PC, Kallenberg CG. Serum amyloid P component binds to late apoptotic cells and mediates their uptake by monocyte-derived macrophages. *Arthritis Rheum* 2003;**48**:248–54
37. Nauta AJ, Daha MR, van Kooten C, Roos A, Lauber R, Bohn E, Krober SM, Xiao YJ, Blumenthal SG, Lindemann RK, Marini P, Wiedig C, Zobywalski A, Baksh S, Xu Y, Autenrieth IB. Schulze Recognition and clearance of apoptotic cells: a role for complement and pentraxins. *Trends Immunol* 2003;**24**:148–54
38. Ruzittu M, Carlá EC, Montinari MR, Maietta G, Dini L. Modulation of cell surface expression of liver carbohydrate receptors during in vivo induction of apoptosis with lead nitrate. *Cell Tissue Res* 1999;**298**:105–12
39. Dini L, Carlà EC. Hepatic sinusoidal endothelium heterogeneity with respect to the recognition of apoptotic cells. *Exp Cell Res* 1998;**240**:388–93
40. Ravichandran KS. Find-me and eat-me signals in apoptotic cell clearance: progress and conundrums. *J Exp Med* 2010;**207**:1807–17
41. Horino K, Nishiura H, Ohsako T, Shibuya Y, Hiraoka T, Kitamura N, Yamamoto T. A monocyte chemotactic factor, S19 ribosomal protein dimer, in phagocytic clearance of apoptotic cells. *Lab Invest* 1998;**78**:603–17
42. Knies UE, Behrensdorf HA, Mitchell CA, Deutsch U, Risau W, Drexler HC, Clauss M. Regulation of endothelial monocyte-activating polypeptide II release by apoptosis. *Proc Natl Acad Sci U S A* 1998;**95**:12322–7
43. Lauber R, Bohn E, Krober SM, Xiao YJ, Blumenthal SG, Lindemann RK, Marini P, Wiedig C, Zobywalski A, Baksh S, Xu Y, Autenrieth IB, Schulze-Osthoff K, Belka C, Stuhler G, Wesselborg S. Apoptotic cells induce migration of phagocytes via caspase-3-mediated release of a lipid attraction signal. *Cell* 2003;**113**:717–30
44. Elliott MR, Chekeni FB, Trampont PC, Lazarowski ER, Kadl A, Walk SF, Park D, Woodson RI, Ostankovich M, Sharma P, Lysiak JJ, Harden TK, Leitinger N, Ravichandran KS. Nucleotides released by apoptotic cells act as a find-me signal to promote phagocytic clearance. *Nature* 2009;**461**:282–6
45. Truman LA, Ford CA, Pasikowska M, Pound JD, Wilkinson SJ, Dumitriu IE, Melville L, Melrose LA, Ogden CA, Nibbs R, Graham G, Combadiere C, Gregory CD. CX3CL1/fractalkine is released from apoptotic lymphocytes to stimulate macrophage chemotaxis. *Blood* 2008;**112**:5026–36
46. Qu X, Zou Z, Sun Q, Luby-Phelps K, Cheng P, Hogan RN, Gilpin C, Levine B. Autophagy gene-dependent clearance of apoptotic cells during embryonic development. *Cell* 2007;**128**:931–46
47. Garg AD, Nowis D, Golab J, Agostinis P. Photodynamic therapy: illuminating the road from cell death towards anti-tumour immunity. *Apoptosis* 2010;**15**:1050–71
48. Korbelik M, Sun J, Cecic I. Photodynamic therapy-induced cell surface expression and release of heat shock proteins: relevance for tumor response. *Cancer Res* 2005;**65**:1018–26
49. Zhou F, Xing D, Chen WR. Dynamics and mechanism of HSP70 translocation induced by photodynamic therapy treatment. *Cancer Lett* 2008;**264**:135–44
50. Korbelik M, Sun J. Photodynamic therapy-generated vaccine for cancer therapy. *Cancer Immunol Immunother* 2006;**55**:900–9
51. Epstein SP, Baer RL, Thorbecke GJ, Belsito DV. Immunosuppressive effects of transforming growth factor beta: inhibition of the induction of Ia antigen on Langerhans cells by cytokines and of the contact hypersensitivity response. *J Invest Dermatol* 1991;**96**:832–7
52. Yang L. TGFbeta, a potent regulator of tumor microenvironment and host immune response, implication for therapy. *Curr Mol Med* 2010;**10**:374–80
53. Geissmann F, Revy P, Regnault A, Lepelletier Y, Dy M, Brousse N, Amigorena S, Hermine O, Durandy A. TGF-beta 1 prevents the non cognate maturation of human dendritic Langerhans cells. *J Immunol* 1999;**162**:4567–75
54. Moore KW, de Waal Malefyt R, Coffman RL, O'Garra A. Interleukin-10 and the interleukin-10 receptor. *Annu Rev Immunol* 2001;**19**:683–765
55. Hagenbaugh A, Sharma S, Dubinett SM, Wei SH, Aranda R, Cheroutre H, Fowell DJ, Binder S, Tsao B, Locksley RM, Moore KW, Kronenberg M. Altered immune responses in interleukin 10 transgenic mice. *J Exp Med* 1997;**185**:2101–10
56. Peters N, Sacks D. Immune privilege in sites of chronic infection: Leishmania and regulatory T cells. *Immunol Rev* 2006;**213**:159–79
57. Massagué J. TGFbeta in cancer. *Cell* 2008;**134**:215–30
58. Tanikawa T, Wilke CM, Kryczek I, Chen GY, Kao J, Núñez G, Zou W. Interleukin-10 ablation promotes tumor development, growth, and metastasis. *Cancer Res* 2012;**72**:420–9
59. Zheng LM, Ojcius DM, Garaud F, Roth C, Maxwell E, Li Z, Rong H, Chen J, Wang XY, Catino JJ, King I. Interleukin-10 inhibits tumor metastasis through an NK cell-dependent mechanism. *J Exp Med* 1996;**184**:579–84
60. Berman RM, Suzuki T, Tahara H, Robbins PD, Narula SK, Lotze MT. Systemic administration of cellular IL-10 induces an effective, specific, and long-lived immune response against established tumors in mice. *J Immunol* 1996;**157**:231–8
61. Fujii S, Shimizu K, Shimizu T, Lotze MT. Interleukin-10 promotes the maintenance of antitumor CD8(+) T-cell effector function in situ. *Blood* 2001;**98**:2143–51

(Received October 1, 2012, Accepted April 6, 2013)